Desalination and Water Treatment
www.deswater.com
doi: 10.5004/dwt.2018.23113

136 (2018) 252–258
December

Optimization of $UV/H_2O_2/Fe_3O_4$ process to remove aniline from aqueous solutions using central composite methodology

Babak Mayahi[a], Mohsen Arbabi[b,*], Sara Hemati[c]

[a]*Isfahan University of Medical Sciences, Deputy of Health, Health Care Center No. 1. Isfahan, Iran, email: babakmayahi@gmail.com*
[b]*Departments of Environmental Health Engineering, School of Health, Shahrekord University of Medical Sciences, Shahrekord, Iran, email: marbabi47@yahoo.com*
[c]*PhD Student of Environmental Health Engineering, School of Health, Shahrekord University of Medical Sciences, Shahrekord, Iran, email: hemati.sara88@yahoo.com*

Received 24 March 2018; Accepted 10 September 2018

ABSTRACT

Aniline with a benzene ring in its structure is a toxic, carcinogenic and mutagenic compound that causes many diseases in humans. Various methods have been developed to remove this pollutant from the environment among which the advanced oxidation has been successful in obtaining higher aniline removal efficiency. In this study, a UV light and Fe_3O_4 nano catalyst were used to remove aniline. In this study, the efficiency of aniline removal was studied as a dependent variable and aniline, hydrogen peroxide and iron nano catalyst concentrations, time and pH were investigated as independent variables. The concentration of aniline was measured by spectrophotometer. The optimization of the process was determined using the response surface method design and the central composite design model. Design Expert software was used to analyze the data. The results showed that the aniline removal efficiency decreased with increase in nano-catalyst concentration, hydrogen peroxide concentration and time and decreased with increasing pH and aniline concentration. To achieve maximum efficiency (78.1%), the optimal values for pH; initial concentration; time; nanoparticle content and H_2O_2 content were 3.2; 101 mg L^{-1}; 50 min; 0.45 g L^{-1} and 31.08 mmol L^{-1}. The results showed that the photo-Fenton process has a desirable ability to remove aniline from aqueous solution at pilot scale. Therefore, it was suggested to study the efficiency of this process as one of the clean and environmentally friendly methods at full scale on real wastewater.

Keywords: Aniline; Iron nanoparticles; Advanced oxidation; Response surface methodology; Central composite design

1. Introduction

Water pollution caused by industrialization, urbanization and population growth is a major issue in the world, especially in developing countries [1]. Aniline is used as an important chemical compound in many fields, including dyeing, rubber, pesticides, plastics and pharmaceutical industries [2–5]. Aniline is classified by the US Environmental Protection Agency (US-EPA) as a priority pollutant [6,7], which has the chemical formula $C_6H_5NH_2$ and has a benzene ring in its structure [1,8]. Aniline is a toxic, mutagenic and carcinogenic compound that converts hemoglobin to methemoglobin and causes diseases such as cyanosis, anemia, appetite loss, weight loss and neurological, renal and hepatic disorders [5,9]. The wastewater containing aniline enters it to the receiving waters, thus its limits in China, Canada and US Environmental Protection Agency were reported as 1 mg, 2.2 mg and 6 µg L^{-1}, respectively [10,11]. Therefore, it is necessary to remove it from aqueous solutions.

In recent years, advanced oxidation processes (AOPs) have been used as efficient methods for obtaining high oxidation efficiency of various types of organic compounds [12]. The UV/H_2O_2 process is one of the advanced oxidation

* Corresponding author.

methods used to remove various types of resistant pollutants [13]. Another advanced oxidation method is processes based on the Fenton reaction, the advantages of which include high efficiency, simple operations and low-cost materials. However, the homogeneous Fenton system can be difficult and expensive due to the presence of a large amount of iron in the water followed by the removal of sludge from the final wastewater [14]. The Fenton-like (ferric iron instead of ferrous iron) can be catalyzed by hydrogenated catalysts, including ferric iron, native or added iron oxides specific transferred metals. Iron oxides such as geothetes (α-FeOOH), hematite (α- Fe_2O_3), magnetite (Fe_3O_4) and ferrihydrite (α- $Fe_{10}O_{15}.9H_2O$) were all capable of catalyzing hydrogen peroxide [15,16]. Among metal nanoparticles, iron nanoparticles (Fe_3O_4) have been more widely considered because of their high frequency, non- toxicity, rapid reaction, and high ability and efficiency [17]. Fe_3O_4 nanoparticles can also be easily removed from the reaction by an external magnet [14].

So far, many studies have been conducted on the removal of aniline by AOPs. The results of Zhao et al. [18] showed that aniline was removed by 23.1% and 67.7% using UV and UV/O_3 processes. In a study conducted by Anotai et al. [19] on aniline by Fenton and electro-Fenton processes, it was found that 38% and 85.9% of aniline were removed, respectively.

Advantages and disadvantages of the present study are summarized as below:

Advantages: 1- Application of two oxidants namely; UV and Fe_3O_4 with together in same times in single reactor, led to increase the production of OH-radicals and will increased removal efficiencies of aniline in shorter time. 2- By using of a magnet to adsorb aniline after degradation by hydroxyl radicals, Fe_3O_4 nano-catalysts are easily separated from the solution, and in this case, the feasibility of process will be increased in full-scale applications. 3- This method has been considered as a clean method due to no secondary contamination and no sludge production.

In full-scale applications, preservation and shading of UV lamps and also need to pretreatment of strong aniline polluted wastewater, may be short comings of this process.

Therefore, the purpose of this study was to evaluate the efficiency of aniline removal by the UV/H_2O_2/Fe_3O_4 process. The synergistic effects of ultraviolet radiation and Fe_3O_4 nanoparticles in the production of hydroxyl radicals ($OH^{\cdot}$) were also investigated.

2. Materials and methods

2.1. Chemicals and materials

Magnetite iron nanoparticles Fe_3O_4 with a particle size of 15–20 nm, a 6 W – middle range – UV-C lamp and aniline, H_2SO_4, NaOH and H_2O_2 (30%) were purchased from US-Nano Corporation, Osram, Germany, and Merck, Germany, respectively.

2.2. Experiment

In this research, AOP, including UV/H_2O_2/Fe_3O_4UV/H_2O_2/Fe_3O_4 was used for aniline removal from synthetic samples.

Stock solution (1,000 mg L^{-1}) of aniline was prepared according to Standard Methods book. Then, standards of stock solution were made at concentrations of 20, 57.7, 112.3 and 150 mg L^{-1}. The amounts of 10, 18.7, 25, 31.3 and 40 mmol of hydrogen peroxide, 0.5, 0.93, 1.25, 1.57 and 2 g of Fe_3O_4 nanoparticles were considered to prepare hydroxyl radicals with UV lamp and the periods of 10, 24.5, 35, 45.5 and 60 min were intended to evaluate the effect of time on the oxidation process. The pH of the solution was adjusted by 0.1% normal sulfuric acid (H_2SO_4) or 0.1% normal sodium hydroxide (NaOH), that is, 3, 5.3, 7, 8.7 and 11. All experiments were carried out in a batch glass reactor with specific volume of 2 L that equipped with a 6 watt UV lamp covered with a quartz tube and mechanical mixer of 120 rpm. The reactor was placed in a wooden chamber with no aperture and in full darkness, and all experiments were carried out at room temperature. The volume of the applied solution was 2 L. 0.45 μm Whatman filter paper (cellulose acetate) was used to isolate nanoparticles from solutions. To measure aniline concentration, a UV-2100 spectrophotometer was used with a wavelength of 230 nm [1,20]. The percentage of aniline removal was calculated by Eq. (1):

$$\text{Removal}(\%) = \frac{C_0 - C_t}{C_0} \times 100 \tag{1}$$

where C_0 and C_t are the initial and final concentrations of aniline, respectively [20–23].

2.3. Experimental design

One of the response surface methodology (RSM) approach, that is widely used in researches, is the central composite design (CCD) [24]. In this study, RSM based on the CCD was used to evaluate the interaction effect on the response function (color removal efficiency) and predict the best response rate [25,26]. This method designates five levels, including +a, +1, 0, –1 and –a. In order to design experiments with a central composite design, minimal and maximum levels were given to Design Expert software and the other levels were determined between the maximum and minimum points by the software [27,28]. The variables in this study included pH (A), H_2O_2 concentration (B), time (C), Fe_3O_4 nanocatalysts concentration (D) and aniline concentration (E). Aniline removal efficiency was the dependent variable in this study. Based on the effects of factors in five levels with five factors and eight repetitions at the central point, the total number of experiments in this design method was 50 tests. Five levels for the factors were shown in Table 1.

Table 1
Variable range based on central composite design

Independent variables	Levels				
	$+\alpha$	1	0	–1	$-\alpha$
pH	11	8.7	7	5.3	3
Amount of H_2O_2 (mmol/L)	40	31.3	25	18.7	10
Time (min)	60	45.5	35	24.5	10
Amount of Fe_3O_4 (g/L)	2	1.75	1.25	0.93	0.5
Concentration of aniline (mg/L)	150	112.3	85	57.7	20

3. Result and discussion

3.1. Characteristics of Fe_3O_4 nanoparticles

The surface morphology of the sorbent was determined by scanning electron microscopy (SEM). The characteristics of Fe_3O_4 nanoparticles are shown in Table 2. Fig. 1 illustrates the SEM of nano-Fe_3O_4 nanoparticles.

3.2. Statistical analysis

In the UV/H_2O_2/Fe_3O_4 process after the effect of variables, a quadratic equation was obtained which was used to predict efficiency and indicated the experimental relationship between variables and efficiency:

$$R\,(\%) = +39.15 - 6.95\,A + 1.84\,B + 12.39\,C + 3.06\,D - 9.87\,E - 0.13\,A \times B + 0.044\,A \times C - 0.003\,A \times D - 0.26\,A \times E - 0.11\,B \times C + 0.25\,B \times D - 0.019\,B \times E - 0.031\,C \times D + 0.54\,C \times E - 0.12\,D \times E + 1.95\,A^2 - 0.58\,B^2 + 0.5\,C^2 - 0.14\,D^2 + 0.2\,E^2 \quad (2)$$

where A is pH, B is the concentration of H_2O_2, C is time, D is iron nanocatalyst and E is aniline concentration. Statistical analysis results are presented in Table 3. Also, the significance of each coefficient is presented by the p-value.

According to Table 3, the amount of p-value for the designed model was <0.00001 which indicates that the proposed model is important for the removal of aniline by the UV/H_2O_2/Fe_3O_4 process so that the p-values smaller than 0.05 and larger than 0.1 in the model indicate whether they are important or irrelevant [29]. The value of R-squared (0.98) means that the model has an acceptable accuracy. Also the predicted and adjusted R-squared were 0.92 and 0.97, respectively, indicating a logical agreement with each other. On the other hand, the adequate precision parameter indicates the ratio of warning to the disorder and if it is greater than 4, it will be acceptable and in this study the value of 34.9 is a desirable value.

In this study with the model presented by the software which is confirmed above, all the parameters were set at maximum level of 76.06 within the design and removal efficiency range. To achieve the maximum efficiency of 76.06%, the optimal values for pH, initial aniline concentration, time, nanoparticle and H_2O_2 contents were 3.2, 101 mg L^{-1}, 50 min, 1.45 g L^{-1} and 31.08 mmol L^{-1}, respectively and these conditions were implemented with three repetitions and a mean efficiency of 78.1% was obtained.

Fig. 2 shows the results of the study as surface diagrams (three dimensional) that is related to the effect of pH, H_2O_2 concentration, time, iron nano-catalyst concentration and aniline concentration on the aniline removal efficiency.

Fig. 2(a) shows the effect of pH and H_2O_2 concentration. As shown in the diagram, with increasing pH, the efficiency was decreased and with increasing H_2O_2 the removal efficiency increased.

Fig. 2(b) represents the effect of the concentration of Fe_3O_4 nano-catalysts and time. According to the diagram, the removal efficiency increased with increasing concentration of Fe_3O_4 nano-catalyst and time.

Fig. 2(c) shows the effect of the concentration of H_2O_2 and aniline nano-catalyst where the removal efficiency was reduced by increasing aniline concentration.

Regression coefficients evaluate the adequacy of the model by residuals (the difference between response and observed values), which is expected to occur according to a normal distribution. Normal probability diagrams (Fig. 3) are suitable graphical methods for judging the normality of the residuals. The observed residuals vs. predicted values are shown in Fig. 2 as normal distribution. The analyzed residuals should have a normal distribution and average deviations from normal state do not have a significant effect on the results. The normal probability diagram for the residuals should be a straight line.

Fig. 3(a) shows the dispersion of residuals and how the residuals follow a normal distribution. In this way, the proximity of the points to the ascending line confirms the assumption that the variance is constant. Fig. 3(b) shows the residuals vs. the predicted values and this diagram presents the residuals based on random dispersion to zero where the higher density of points around the graph shows the constant variance, the correlation between quantities and distribution of the observed values around the regression. Fig. 3(c) specifies the residuals for the corresponding observations, and this diagram shows that the residuals oscillate in the form of a random pattern across the midline where the error percentage will be reduced by less data dispersion [25,26].

Perturbation diagram is shown in Fig. 4. In this diagram, the effects of all factors on the central point are compared. The perturbation diagram helps to compare all the factors at a specific point in the design space [30]. As can be seen, among the five factors of pH (A), H_2O_2 concentration (B), time (C), nano-catalyst concentration (D) and aniline concentration (E)

Table 2
Characteristics of Fe_3O_4 nanoparticles

Color	Dark brown
Purity (%)	98
Nanoparticle size (nm)	20–30
Special surface area (g/m^2)	53

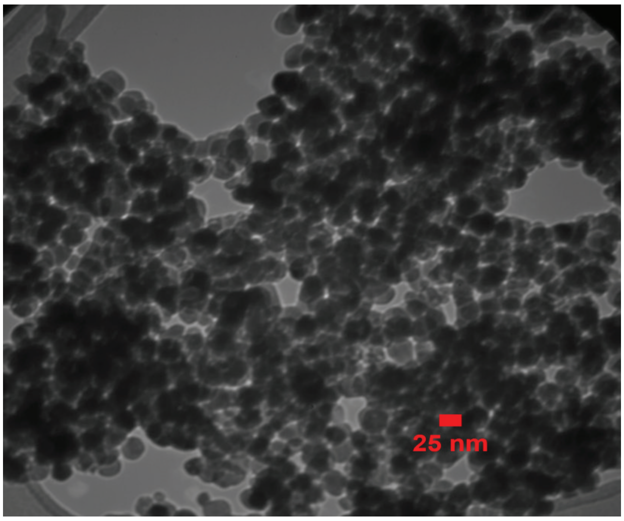

Fig. 1. SEM image of the Fe_3O_4 nanoparticle.

Table 3
Analysis of variance (classical sum of squares – type II)

Source	Sum of squares	df	Mean square	F value	p-value Probability > F
Model	13,810.3	20	690.66	75.95	<0.0001
pH A	2,092.48	1	2,092.48	230.11	<0.0001
H_2O_2 (mmol L^{-1}) B	146.59	1	146.59	16.12	<0.0004
Time (min) C	6,651.1	1	6,651.1	731.41	<0.0001
Fe_3O_4 (g L^{-1}) D	405.31	1	405.31	44.57	<0.0001
Dye (mg L^{-1}) E	4,219.33	1	4,219.33	463.99	<0.0001
AB	0.56	1	0.56	0.062	0.8055
AC	0.063	1	0.063	0.003	0.9342
AD	0.004	1	0.004	0.005	0.9972
AE	2.22	1	2.22	0.24	0.6253
BC	0.4	1	0.4	0.044	0.8361
BD	1.98	1	1.98	0.22	0.6443
BE	0.011	1	0.011	0.003	0.9722
CD	0.03	1	0.03	3.3	0.9546
CE	9.31	1	9.31	1.02	0.32
DE	0.45	1	0.45	0.049	0.8262
A^2	211.6	1	211.6	23.27	<0.0001
B^2	18.64	1	18.64	2.05	0.1629
C^2	13.87	1	13.87	1.53	0.2267
D^2	1.06	1	1.06	0.12	0.7353
E^2	2.3	1	2.3	0.25	0.6187
Residual	261.71	29	9.09	–	–
Lack of Fit	263.41	22	11.97	277.9	<0.0001
Pure error	0.3	7	0.043	–	–
Corrected total	14,077.01	49	690.66	–	–

time and aniline concentration have the most effect on the removal efficiency.

In this study, with increasing pH the removal efficiency decreased. Liu et al. [31] reported that the highest aniline removal efficiency was obtained at a pH between 3 and 4 and, with increasing pH, the removal efficiency decreased. In fact, with increasing pH, the catalytic activity decreases, which results from the precipitation of iron hydroxides and the loss of its catalytic activity and at the same time by reducing pH lower than 3, the H^+ ions act as inhibitors and affect hydroxyl radicals [31]. In other words, the photocatalytic reaction has the highest productivity in acidic pH. This is due to the presence of more hydrogen ions in the acidic environment acting as a precursor to hydrogen radicals. These radicals then form the InlineEqn1 radicals by reacting with the oxygen present in the solution and ultimately lead to the production of $OH^{\cdot}$ radicals [32]. In confirmation of the present study, the study by Mandal et al. [33] showed that in the photo-Fenton process, hydroxyl radicals are produced by the reaction between Fe^{2+} and H_2O_2 at an optimal pH of 2.7. Also, the results of the study by Shams-khoramabadi et al. [34] showed that at pH = 5, the maximum efficiency of aniline removal was obtained and by decreasing the pH, the efficiency of the process decreased.

As it was observed with increasing H_2O_2 from 10 to 40 mmol L^{-1}, the removal efficiency increased. The concentration changes of this compound as a major factor in the production of $OH^{\cdot}$ has a great effect on the efficiency of aniline removal. In a study by Yazdanbakhsh [35] on the phenol removal by the Fenton-like process, the increase in efficiency was attributed to the increase in H_2O_2 content and by increasing H_2O_2 the number of hydroxyl radicals increases, they have better accessibility and the removal efficiency increases. Aleix et al. [36] reported that the increase in H_2O_2 concentration increased the aniline removal rate. Malakootian and Asadi [37] argued that with increasing H_2O_2 concentration, the phenol removal efficiency increased. They also reported that with excessive increase in concentrations of hydrogen peroxide; this substance is decomposed into oxygen and water and hydroxyl radicals are combined together. Therefore, the excessive presence of hydrogen peroxide decreases the removal efficiency. They stated the reason as the reaction between additional H_2O_2 with hydroxyl radical and production of less-reactive radicals [37]. Similar results were also reported by Dehghani et al. [38].

In this study, the removal efficiency increased with increasing concentration of Fe_3O_4 nano-catalyst. In fact with increasing the concentration of the nano-catalyst, more active unsaturated active surface is available and the production of hydroxyl radicals increases [39]. The results of this study are consistent with the study by Kadirova et al. [40] on the effect of loading Fe_2O_3 in photocatalytic decomposition of methylene blue. It has been stated in this study that with increasing catalyst concentration, the number of absorbed photons

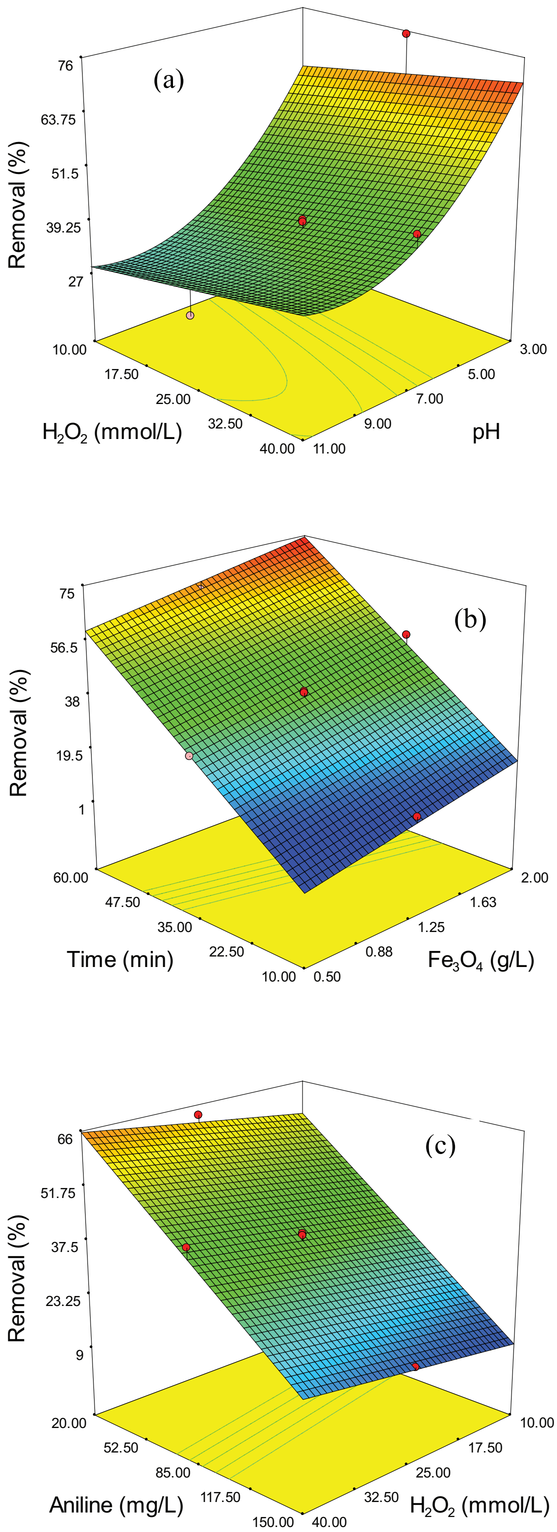

Fig. 2. Interactive effect of the studied variables on the aniline removal efficiency. (a) pH and H_2O_2 (dye concentration: 85 mg L^{-1}, time: 35 min, Fe_3O_4 concentration: 1.25 g L^{-1}); (b) concentration of nano-catalysts and time (pH: 7, H_2O_2 concentration: 25 mmol L^{-1}, aniline concentration: 85 mg L^{-1}); (c) aniline and H_2O_2 concentrations (time: 35 min, pH: 7, Fe_3O_4 concentration: 1.25 g L^{-1}).

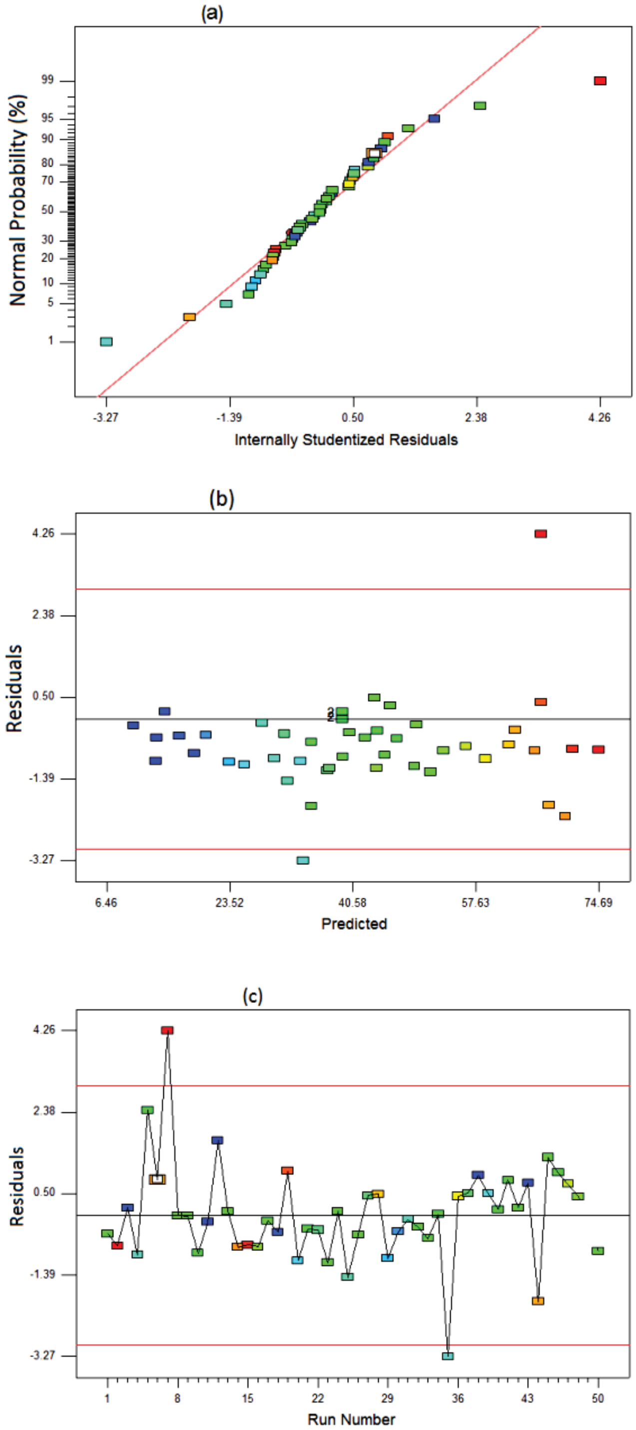

Fig. 3. Diagram of aniline removal efficiency residual. (a) Normal distribution of residuals; (b) predicted values vs. residual values; (c) residual values vs. observed values.

increases and eventually leads to an increase in the number of active sites on the photocatalyst surface. As a result, with increasing Fe_2O_3, the photocatalytic decomposition of methylene blue increases [40]. In Zhang et al. [41] it was found that that with increasing nano-catalyst from 0 to 5 g L^{-1}, the production of hydroxyl radicals and consequently the removal efficiency of phenolic compounds increased. Gogoi et al. [42]

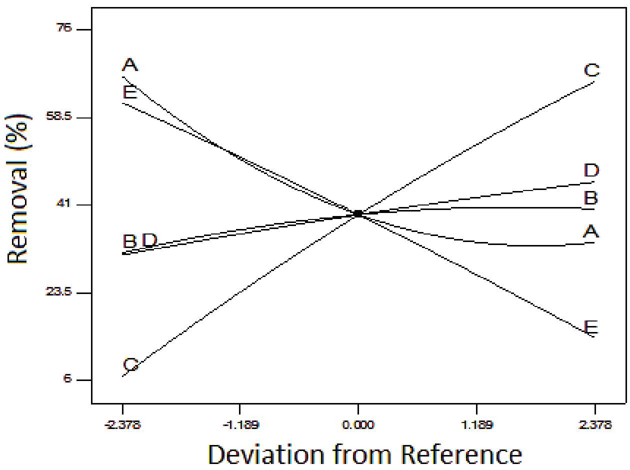

Fig. 4. Perturbation diagram of aniline removal.

concluded that by increasing the CaO_2/Fe_3O_4 catalyst to 50 mg in the acidic environment, more catechol is likely to be decomposed the reason of which is attributed to its small particles, more active sites and larger Fe_3O_4 contact surface.

With increasing radiation time, the removal efficiency increased. In fact, with increasing time, hydroxyl radicals have more time to react with UV rays. Increasing time also increases the interactions of hydroxyl radicals with organic matter molecules [43]. The results of the study by Karthikeyan et al. [44] on aniline removal by the heterogeneous Fenton process showed that the removal efficiency was increased by increasing the time from 10 to 60 min. In a study conducted on absorption and decomposition of methylene blue with hematite-active carbon under UV by Kadirova et al. [40] it has been shown that with increasing time, the removal efficiency has increased. Similar results were obtained by Lofrano [45].

In this study, it was observed that with increasing the initial concentration of aniline from 20 to 150 mg L^{-1}, the removal efficiency decreased. In other words, the removal efficiency is inversely related to the pollutant concentration. This is due to the fact that although aniline concentration increases, the hydroxyl radicals do not increase as a result of it. Therefore, the low ratio of hydroxyl radicals reduces the removal efficiency [46]. The results of Sanchez et al. [47] on phenol removal by iron catalyst were consistent with the results of this study based on the fact that the removal efficiency is reduced by increasing the pollutant concentration.

The results of the study by Rahdar and Sh [48] showed that with increasing aniline concentration, the removal efficiency decreased from 50 to 150 mg L^{-1}. Similar results were also reported by Pirsaheb et al. in 2017 [49].

4. Conclusions

In this research, the parameters affecting advanced oxidation (aniline concentration, Fe_3O_4 nano-catalyst concentration, H_2O_2 concentration, time and pH) were investigated for the removal of aniline from synthetic solution and the results showed that increasing the aniline concentration and pH had negative effect on the removal efficiency and increasing time, hydrogen peroxide and the concentration of iron nanoparticles had a direct effect on the removal efficiency. The method used in this achieved similar aniline removal efficiency in shorter time than other methods of reducing aniline pollutant from aqueous solutions. On the other hand, Fe_3O_4 nano-catalysts are easily separated from the solution by a magnet after aniline degradation by hydroxyl radicals and the use of this method is considered as a clean method due to no secondary contamination and no sludge production. Therefore, it is recommended that this process can be applied to remove aniline at larger scales.

Competing interests

The authors declare that they have no competing interests.

Acknowledgments

The authors are grateful to Deputy of Research and Technology of Shahrekord University of Medical Sciences (SKUMS) for financial support (Project No. 2867) and laboratory assistance of the Department of Environmental Health and Engineering, School of Health, SKUMS.

References

[1] H. Basiri, H. Nourmoradi, F. Mohammadi moghadam, K. Moghadam, J. Mohammadian, Y. Khaniabadi, Removal of aniline as a health-toxic substance from polluted water by aloe vera waste-based activated carbon, Der Pharma Chem., 11 (2015) 149–155.

[2] N. Hankins, N. Hilal, First Oxford and Nottingham Water and Membranes Research Event 2–4 July 2006, Oxford, UK Feasibility study of the treatment of aniline hypersaline wastewater with a combined adsorption/bio-regeneration system, Desalination, 227 (2008) 139–149.

[3] X. Lin, J. Zhang, X. Luo, Y. Zhou, Removal of aniline using lignin grafted acrylic acid from aqueous solution, J. Chem. Eng., 172 (2011) 856–863.

[4] H. Al-Johani, M.A. Salam, Kinetics and thermodynamic study of aniline adsorption by multi-walled carbon nanotubes from aqueous solution, J. Colloids Interface Sci., 360 (2011) 760–767.

[5] G.Q. Wu, X. Zhang, H. Hui, Q. Zhang, Y. Dai, Adsorptive removal of aniline from aqueous solution by oxygen plasma irradiated bamboo based activated carbon, J. Chem. Eng., 185 (2012) 201–210.

[6] R. Hu, S. Dai, D. Shao, A. Alsaedi, B. Ahmad, X. Wang, Efficient removal of phenol and aniline from aqueous solutions using graphene oxide/polypyrrole composites, J. Mol. Liq., 203 (2015) 80–89.

[7] M. Long, W. Cai, J. Cai, B. Zhou, X. Chai, Y. Wu, Efficient photocatalytic degradation of phenol over $Co_3O_4/BiVO_4$ composite under visible light irradiation, J. Phys. Chem, 110 (2006) 20211–20216.

[8] J. Anotai, Ch. Su, Y. Tsai, M. Lu, Effect of hydrogen peroxide on aniline oxidation by electro-Fenton and fluidized-bed Fenton processes, J. Hazard. Mater., 183 (2010) 888–893.

[9] S.P. Kamble, S. Sawant, J. Schouten, Photocatalytic and photochemical degradation of aniline using concentrated solar radiation, J. Chem. Technol. Biotechnol., 78 (2003) 865–872.

[10] J. Liu, J. Guan, M. Lu, Q. Kan, Zh. Li, Hemoglobin immobilized with modified “fish-in-net” approach for the catalytic removal of aniline, J. Hazard. Mater., 217 (2012) 156–163.

[11] Y. Han, X. Quan, Sh. Chen, H. Zhao, Ch. Cui, Electrochemically enhanced adsorption of aniline on activated carbon fibers, Sep. Purif. Technol., 50 (2006) 365–372.

[12] G. Zhang, F. Yang, L. Liu, Comparative study of Fe^{2+}/H_2O_2 and Fe^{3+}/H_2O_2 electro-oxidation systems in the degradation of amaranth using anthraquinone/polypyrrole composite film modified graphite cathode, J. Electroanal. Chem., 632 (2009) 154–161.

[13] A. Zuorro, M. Fidaleo, R. Lavecchia, Response surface methodology (RSM) analysis of photodegradation of sulfonated diazo dye Reactive Green 19 by UV/H_2O_2 process, J. Environ. Manage., 127 (2013) 28–35.

[14] K. Chen, G. Wang, W. Li, D. Wang, L. Lu, Application of response surface methodology for optimization of Orange II removal by heterogeneous Fenton-like process using Fe_3O_4 nanoparticles, Chin. Chem. Lett., 25 (2014) 1455–1460.

[15] A. Rezaee, S. Jorfi, A. Jaafarzadeh Haghighifard, Application of Fenton-like process using iron nano oxides for pyrene removal from contaminated soils, Iran. J. Health. Environ., 7 (2014) 301–314.

[16] M. Usman, P. Faure, C. Ruby, Kh. Hanna, Remediation of PAH-contaminated soils by magnetite catalyzed Fenton-like oxidation, Appl. Catal. Environ., 117 (2012) 10–17.

[17] M. Bahrami, S. Borumandnasab, H. Kashkuli, A. Babaei, Synthesis of magnetite nanoparticles (Fe_3O_4) and its efficiency in cadmium removal from aqueous solutions, Water Wastewater, 3 (2012) 54–62.

[18] G. Zhao, X. Lu, Y. Zhou, Aniline degradation in aqueous solution by UV-aeration and UV-microO_3 processes: efficiency, contribution of radicals and byproducts, Chem. Eng. J., 229 (2013) 436–443.

[19] J. Anotai, M.-C. Lu, P. Chewpreecha, Kinetics of aniline degradation by Fenton and electro-Fenton processes, Water Res., 40 (2006) 1841–1847.

[20] R.S. Bose, S. Dey, S. Saha, Ch. Ghosh, M. Chaudhuri, Enhanced removal of dissolved aniline from water under combined system of nano zero-valent iron and *Pseudomonas putida*, Sustain. Water Resour. Manage., 2 (2016) 143–159.

[21] A. Chaleshtori, F. Mohammadimoghadam, M. Sadeghi, R. Rahimi, S. Hemati, Removal of Acid Red 18 (Azo-Dye) from aqueous solution by adsorption onto activated charcoal prepared from almond shell, J. Environ. Sci. Manage., 20 (2017) 9–16.

[22] S. Nourozi, R. Zare-Dorabei, Highly efficient ultrasonic-assisted removal of methylene blue from aqueous media by magnetic mesoporous silica: experimental design methodology, kinetic and equilibrium studies, Desal. Wat. Treat., 85 (2017) 184–196.

[23] M.S. Tehrani, R. Zare-Dorabei, Competitive removal of hazardous dyes from aqueous solution by MIL-68 (Al): derivative spectrophotometric method and response surface methodology approach, Spectrochim. Acta, Part A, 160 (2016) 8–18.

[24] R. Zare-Dorabei, S. Ferddowsi, A. Barzin, A. Tadjarodi, Highly efficient simultaneous ultrasonic-assisted adsorption of Pb(II), Cd(II), Ni(II) and Cu (II) ions from aqueous solutions by graphene oxide modified with 2,2′-dipyridylamine: central composite design optimization, Ultrason. Sonochem., 32 (2016) 265–276.

[25] M.B. Kasiri, A.R. Khataee, Photooxidative decolorization of two organic dyes with different chemical structures by UV/H_2O_2 process: experimental design, Desalination, 270 (2011) 151–159.

[26] M. Arbabi, S. Hemati, Z. Shamsizadeh, A. Arbabi, Nitrate removal from aqueous solution by almond shells activated with magnetic nanoparticles, Desal. Wat. Treat., 80 (2017) 344–351.

[27] K. Dashtian, R. Zare-dorabi, R. Jafarinia, M. Tehrani, Application of central composite design for optimization of preconcentration and determination of La (III) ion in water samples using the SBA-15-HESI and SBA-15-HESI-Fe_3O_4-NPs sorbents, J. Environ. Chem. Eng., 5 (2017) 5233–5240.

[28] F. Nemati, R. Zare-dorabi, M. Hosseini, M. Ganjali, Fluorescence turn-on sensing of thiamine based on Arginine – functionalized graphene quantum dots (Arg-GQDs): central composite design for process optimization, Sens. Actuators, B, 255 (2018) 2078–2085.

[29] V.A. Sakkas, M. Ialam, C. Stalikas, T. Albanis, Photocatalytic degradation using design of experiments: a review and example of the Congo red degradation, J. Hazard. Mater., 175 (2010) 33–44.

[30] B.K. Körbahti, M.A. Rauf, Determination of optimum operating conditions of carmine decoloration by UV/H_2O_2 using response surface methodology, J. Hazard. Mater., 161 (2009) 281–286.

[31] Q. Liu, Y.X. Liu, X. Lu, Combined photo-Fenton and biological for the treatment of anilin wastewater, Procedia Environ. Sci., 12 (2012) 341–348.

[32] M. Aslam, Evaluation of sunlight induced structural changes and their effect on the photocatalytic activity of V_2O_5 for the degradation of phenols, J. Hazard. Mater., 286 (2015) 127–135.

[33] A. Mandal, K. Ojha, K. De.Asim, S. Bhattacharjee, Removal of catechol from aqueous solution by advanced photo-oxidation process, Chem. Eng. J., 102 (2004) 203–208.

[34] G. Shams-khoramabadi, Aniline degradation using advanced oxidation process by UV/peroxy disulfate from aqueous solution, Int. J. Eng. Trans. B: Appl., 30 (2017) 684.

[35] A. Yazdanbakhsh, Investigation of combined process of coagulation and Fenton-like advanced oxidation to remove the antibiotic clarithromycin COD synthetic wastewater, J. Lorestan Univ. Med. Sci., 13 (2011) 7–16.

[36] A. Benito, A. Penades, J. Liberia, R. Gonzalez, Degradation pathways of aniline in aqueous solutions during electro-oxidation with BDD electrodes and UV/H_2O_2 treatment, Chemosphere, 166 (2017) 230–237.

[37] M. Malakootian, M. Asadi, Efficiency of fenton oxidation process in removal of phenol in aqueous solutions, water and wastewater, 3 (2011) 47–52.

[38] S. Dehghani, A. Jafari, M. Farzadkia, M. Gholami, Sulfonamide antibiotic reduction in aquatic environment by application of fenton oxidation process, Iran. J. Environ. Health Sci. Eng., 10 (2013) 29.

[39] H. Chen, Zh. Zhang, Z. Bai, Heterogeneous fenton-like catalytic degradation of 2,4-dichlorophenoxyacetic acid in water with FeS, J. Chem. Eng., 273 (2015) 481–489.

[40] Z.C. Kadirova, K. Katsumata, K. Okada, Adsorption and photodegradation of methylene blue with Fe_2O_3-activated carbons under UV illumination in oxalate solution, J. Environ. Chem. Eng., 2 (2014) 2026–2036.

[41] S. Zhang, X. Zhau, Y. Cai, G. Jiang, Superparamagnetic Fe_3O_4 nanoparticles as catalysts for the catalytic oxidation of phenolic and aniline compounds, J. Hazard. Mater., 167 (2009) 560–566.

[42] A. Gogoi, M. Navgire, P. Gogoi, Fe_3O_4-CeO_2 metal oxide nanocomposite as a Fenton-like heterogeneous catalyst for degradation of catechol, Chem. Eng., 311 (2017) 153–162.

[43] B. Kayan, B. Gözmen, Degradation of Acid Red 274 using H_2O_2 in subcritical water: application of response surface methodology, J. Hazard. Mater., 201 (2012) 100–106.

[44] S. Karthikeyan, V. Gupta, A. Titus, G. Sekaran, A new approach for the degradation of high concentration of aromatic amine by heterocatalytic Fenton oxidation: kinetic and spectroscopic studies, J. Mol. Liq., 173 (2012) 153–163.

[45] G. Lofrano, Advanced oxidation of catechol: a comparison among photocatalysis, Fenton and photo-Fenton processes, Desalination, 249 (2009) 878–883.

[46] E. Azizi, M. Gayebzade, K. Shrafi, M. Pirsaheb, Oxidation of aniline with photo-Fenton advanced oxidation process from aqueous solutions in batch reactor, Techn. J. Eng. Appl. Sci., 5 (2015) 12–16.

[47] I. Sanchez, F. Stuber, J. Font, Elimination of phenol and aromatic compounds by zero valent iron and EDTA at low temperature and atmospheric pressure, Chemosphere, 68 (2007) 338–344.

[48] S. Rahdar, A. Sh, Removal of phenol and aniline from aqueous solutions by using adsorption on to *Pistacia terebinthus*: study of adsorption isotherm and kinetics, J. Health Res. Commun., Winter, 2 (2017) 35–45.

[49] M. Pirsaheb, B. Shahmoradi, H. Hossini, Gh. Ashraf, Photocatalytic degradation of aniline from aqueous solutions under sunlight illumination using immobilized Cr: ZnO nanoparticles, Sci. Rep., 7 (2017) 1473.